Two regimes of slow light losses revealed by adiabatic reduction of group velocity

R.J.P. Engelen[1], D. Mori[2], T. Baba[2], and L. Kuipers[1]

[1] *Center for Nanophotonics, FOM Institute for Atomic and Molecular Physics (AMOLF), Kruislaan 407, 1098 SJ Amsterdam, The Netherlands*

[2] *Yokohama National University, Department of Electrical and Computer Engineering, 79-5 Tokiwadai, Hodogayaku, Yokohama 240-8501, Japan*

(Dated: April 2, 2008)

Abstract

The losses in a photonic crystal waveguide were measured with a near-field microscope in the group velocity range of $c/7$ up to $c/100$. The waveguide under investigation was chirped so that the group velocity becomes position dependent and decreases adiabatically as the light propagates further into the waveguide. The position at which a given group velocity is obtained can therefore be tuned by controlling the optical frequency. By using a range of frequencies, we can investigate the losses for a specific group velocity for many different realizations of unintentional disorder and thereby obtain the realization-averaged behavior. When all group velocities are considered together the losses are found to scale proportional to $v_g^{-\alpha}$, with an unusual loss exponent of α=2.9$\pm$0.3. Our measurements show that for group velocities v_g below $c/30$, the modal pattern becomes irregular indicative of multiple scattering. Both findings show that the usual perturbative approach to describe the propagation of light in a photonic crystal waveguide with fabrication disorder breaks down at lower group velocities.

PACS numbers: 42.70.Qs, 42.82.Et, 68.37.Uv, 42.25.Fx

Photonic crystals (PhCs) consist of a periodic arrangement of dielectric materials, usually with a high refractive index contrast. In a PhC with properly chosen geometry and materials, light can be strongly influenced by the periodic structure. Numerous interesting properties have been reported over the years, like photonic bandgaps [1], negative refraction [2] and super-lensing [3]. One of the intriguing properties of PhCs is that light can be made to propagate with low group velocities at specific optical frequencies [4, 5]. This 'slow light' can enhance nonlinear effects [6], useful for future on-chip all-optical switching.

In two-dimensional photonic crystal waveguides, light can in theory propagate without losses [7]. However, unavoidable structural imperfections like variations in hole diameter or shapes, roughness of the interfaces of the structure and/or slight displacement of the holes will result in coupling out of the waveguide mode, thus inducing loss. We will refer to these imperfections as the disorder in the structure. The major loss channels resulting from the disorder are out-of-plane radiation losses and scattering in the backward direction in the waveguide. Since slow light propagation is intrinsically linked to a very strong interaction with the lattice in which the waveguide is embedded, the losses per unit length increase with decreasing group velocity [8]. Although the disorder created by the structural imperfections is disadvantageous for efficient guiding of light, it can give rise to interesting optical transport phenomena involving multiple scattering [9, 10].

There has been significant effort to determine how the losses in photonic crystal waveguides (PhCWs) scale with the group velocity. Hughes *et. al.* [8] suggested in a theoretical study, that the total losses scale proportional to v_g^{-2}, with v_g being the group velocity of light in the waveguide. Crucial to this study and alike [8, 11], is that the disorder is considered to be a small perturbation on the geometry of the waveguide. The disorder therefore hardly affects the propagation of light apart from the losses scattered out of the mode and the optical properties can therefore be described by the properties of the unperturbed system. There have been a few studies that attempted to elucidate the scaling of the losses experimentally [12–14]. In these studies several waveguides with different lengths are fabricated. By comparing the transmission spectra of the structures for the different lengths, the losses may be determined. For such a study it is crucial that only the waveguide length differs and the mean optical properties are exactly equal. The reported results in Refs. [12–14] range between a proportionality of the losses with $v_g^{-1/2}$ and v_g^{-2}, corresponding to loss exponents (α) of 0.5 and 2, respectively.

Here we investigate the propagation of light and the losses directly by monitoring the optical field in a PhCW en route, with a phase-sensitive near-field microscope. The waveguide under investigation is a so-called chirped waveguide: the hole radius is gradually increased along the propagation direction. As a result, the light slows down adiabatically, which leads to a position-dependent group velocity. By changing the optical frequency, the position in the waveguide for which a specific group velocity occurs can be controlled, with each position having its own local realization of unintentional disorder. We show by visualization of the modal pattern as well as a quantitative analysis of the losses averaged over many realizations of the disorder, that a perturbative approach to dealing with disorder breaks down at low group velocities, in our case below $c/30$, as in this slow-light regime multiple scattering becomes important.

Figure 1 shows a schematic of the waveguide under investigation. A PhCW is created by removing a single row of holes in the photonic crystal lattice [15, 16]. From left to right the hole radius is linearly increased, resulting in a chirped PhCW [17]. We used an air-bridge structure with a 210 nm thick silicon membrane with a hexagonal lattice of air holes with a 456 nm period (a). The hole radius increases linearly from 142 nm to 150 nm over a length of 300 lattice periods, with typical local fabrication variations in diameter of approximately 3 nm. A portion of the dispersion relation calculated by 3D FDTD calculations is presented in Fig. 1, for different sections of the PhCW. In these calculations each section is treated as if it were infinitely long, i.e., with a constant hole radius. In the dispersion relation, the waveguide mode flattens as the wavevector approaches the Brillouin zone boundary at k=0.5 (in units of $2\pi/a$), at which the group velocity ($v_g \equiv \mathrm{d}\omega/\mathrm{d}k$) is zero.

As the hole size increases, the waveguide mode in the dispersion relation shifts to higher frequencies. As a result, light with a certain optical frequency (dashed line in Fig. 1) is allowed to propagate in section I and II. In section III, there is no longer any supported propagating mode for the specified frequency due to the shift of the the local dispersion relation caused by the larger hole radii in this section. Due to the change in hole radii, the group velocity of the light in the PhCW becomes dependent on position. For the frequency range of the guided mode shown in Fig. 1, this leads to a reduction of the group velocity along the propagation direction until the waveguide no longer allows propagation (section III). We will refer to the region were light is propagating with $v_g < c/20$ as the cut-off region. This region corresponds to group indices (defined as $n_g = c/v_g$) above 20. After this region,

the light must either have been reflected back towards the input, or have been scattered out-of-plane.

The optical field inside the waveguide was measured using a phase-sensitive near-field microscope [18]. In this microscope, we scan a near-field probe over the sample at approximately 10 nm height. A small portion of the optical field in the sample couples to the probe [19]. By scanning the probe over the surface we can map the electric (E-)field distribution in the waveguide. Figure 2a shows the amplitude of the E-field picked up in a near-field measurement at ω=0.2961. The waveguide is oriented horizontally, centered around y=2.8 a. The light is incident from the left. We observe that the modal pattern does not change dramatically up to x=190 a. In the cut-off region ($190a < x < 250a$), the pattern broadens laterally and becomes irregular along the propagation direction.

With our near-field microscope we also recovered the phase of the propagating light. By analyzing the phase evolution over 9 lattice periods, the dominant or 'local' wavevector was determined. For the measurement at ω=0.2961, the 'local' wavevector is plotted versus position in Fig. 2b. The expected 'local' wavevector, based on the theoretical dispersion relation, is depicted in red in Fig. 2b. The results for 25 measurements, each at a different optical frequency, all show very good correspondence with the results obtained from the calculated dispersion relation. By exploiting the correspondence between experiment and calculations, we determined the group velocity v_g as a function of position x from the calculated data. The result is depicted in Fig. 2c and shows that the group velocity is 0.12 c at x=0 and gradually decreases, until it reaches zero at x=248.

In order to analyze the experimental data, we summed the intensity ($|E|^2$) of the measurement in Fig. 2a along the y-direction in order to suppress the effect of mode pattern differences so that the energy of the mode can be determined as a function of position along the propagation direction. The thus obtained energy as a function of position is depicted in Fig. 2d. The energy has a short-range oscillation due to two effects: the Bloch wave character of the guided mode [20] and interference of forward propagating and reflected light. The detected intensity shows dramatic changes in the cut-off region ($190a < x < 250a$): the intensity increases, becomes irregular and drops to zero when x is larger.

When we repeat the experiment at different optical frequencies, we observe qualitatively the same results: a gradual increase of the energy at larger propagation distances and an irregular pattern for positions where $v_g < 30$. The first, expected difference is a shift in

position with respect to the measurement at ω=0.2961, as can be seen in Figs. 2e and 2f for ω=0.2973 and ω=0.2950, respectively. Note that these are measurements on the same waveguide and the same measurement area. The position were light stops propagating is clearly dependent on frequency, since these positions are $x \simeq 300$ for ω=0.2973 and $x \simeq 175$ for ω=0.2950. For all 25 optical frequencies used in this investigation, we observe that the mode pattern becomes irregular in the cut-off region. The pattern is different for each frequency, despite the small increments in frequency ($\Delta\omega < 0.07\%$) used. The irregularities in the mode patterns are attributed to local imperfections in the waveguide geometry. Please note that the local imperfections are very small and can hardly be resolved with a good scanning electron microscope. The fact that the shape of the irregularity changes dramatically when a different local realization of the disorder is probed with the same low group velocity, e.g., compare Figs. 2a and 2f, is a fingerprint for multiple scattering [21].

In order to properly quantify the relation between group velocity and losses, one needs to average over the many realizations of the local disorder underlying the losses. This necessity becomes particularly clear considering the large irregularities observed in the cut-off region. We therefore averaged our analysis over 25 measurements, with different optical frequencies. Since the shift in frequency of the local dispersion relation is linear with respect to position, the relation of group velocity and position is the same for each frequency, apart from a shift in position. By averaging over many frequencies, we average over different realizations of the disorder within a single sample, while the coupling of light into the waveguide remains unchanged.

Figure 3 depicts the intensity picked up by the probe as a function of the group index, averaged over 25 effective realizations. It shows that the detected intensity increases linearly with group index between n_g=7 and n_g=15. At higher group indices the increase of the detected intensity slows down until the intensity reaches a maximum at n_g=50. When the group index increases further, the probed intensity decreases.

We attribute the nearly linear increase of the intensity between n_g=7 and n_g=15 in Fig. 3 to an increase of the E-field amplitude in the waveguide. The intensity ($|E|^2$) of light in photonic crystal waveguides is expected to be proportional to the group index [6]. To the best of our knowledge, our measurement is the first direct observation that the local energy density increases in a photonic crystal as the group velocity decreases. The energy in the chirped waveguide therefore increases as a result of the increase in group index, while the

losses are still modest. At larger group indices the waveguide losses increase, finally resulting in a decrease of the measured intensity.

From these measurements, we can recover the losses in the waveguide as a function of group velocity. We can describe the intensity in the waveguide according to Lambert-Beer's law:

$$I(x + \mathrm{d}x) = I(x)\mathrm{e}^{-An_g^\alpha(x)\mathrm{d}x}, \tag{1}$$

describing that an infinitesimal increase in position is accompanied by a loss which scales with n_g^α, with n_g a function of x. We keep the loss exponent α constant for all n_g, in order to compare our quantitative results with that of others. Using the assumption that $|n_g^\alpha(x)\mathrm{d}x| \ll 1$, the above equation leads to

$$I(x) = I(0)\exp[-A\int_0^x n_g^\alpha(x')\ \mathrm{d}x'], \tag{2}$$

with A being a loss coefficient, $I(0)$ the intensity input in the waveguide. When we want to fit this relation to the measured results, the integral needs to be evaluated, but since $n_g(x)$ can not be approximated with a low-order polynomial, we have evaluated the integral in Eq. 2 numerically.

In the fit of Eq. 2 to the measured position-dependent intensity, the fit parameters were the loss exponent α, the loss coefficient A and $I(0)$. The resulting fit is shown in Fig. 3. We find a close agreement with the measured results using α=2.84. The fit has a goodness R^2 of 0.97 [22]. Note that an R^2 value of 1 represents a perfect overlap with the data. Following the fit result, the loss at n_g=7 would be 1.8 dB/mm, which is a typical loss figure for these waveguides [12, 13]. By allowing R^2 values down to 0.95, we obtain a loss exponent α of 2.9 ± 0.3. Clearly, if a single exponent $\alpha = 2$ is forced to describe also the group velocity regime (green curve in Fig. 3), the result is unsatisfactory having an R^2 of 0.82.

The found exponent of 2.9 ± 0.3 is still significantly larger than the exponent predicted and measured previously [8, 12, 14]. The large exponent cannot be attributed to a non-adiabatic transition to lower group velocity due to the design of the chirped waveguide. In fact, recent publications [23, 24] have shown that a transition to velocities of $v_g < c/100$ can be very efficient in chirped waveguides, even within in 3 or 4 lattice spacings, compared to the ~ 200 lattice spacings used in this investigation.

The large discrepancy between theoretical predictions and the experimental observations can be explained as follows. The theoretical predictions are based on perturbation theory,

which does not include multiple scattering phenomena. The multiple scattering leads to a change in the propagation properties, for example by the formation of highly localized resonances (see arrow in Fig. 2f). We discriminate two regimes of slow light propagation. In the first regime the waveguide modes are well behaved and can be described with existing theory. In the second regime, at lower v_g, multiple scattering becomes important, which is no longer described by existing theory. The group velocity for which the transition between the two regimes occurs will depend on the quality of the fabrication: the higher the quality, the smaller the group velocity for which multiple scattering becomes important. In our investigation, this transition occurs at roughly $c/30$.

In conclusion, our measurements on a chirped photonic crystal waveguide shows that the detected intensity increases in a near-field microscope as the group velocity in the waveguide decreases. The increase is proportional to the increase of the electromagnetic energy density in the waveguide. As the light propagates further, the group velocity decreases further and a decrease in detected intensity due to increased waveguide losses is observed. In the area were the losses increase, the modal pattern breaks up and becomes irregular. Using the experimental data, we recovered that the losses scale proportional to $v_g^{-\alpha}$, with α=2.9 $\pm$ 0.3 when a single exponent is used to describe all the losses together: significantly larger than expected based on a perturbative treatment of the disorder. From our observations we conclude that two regimes should be considered when describing the propagation of light in a photonic crystal waveguide. One in which the group velocities are relatively high and which is well described by the usual perturbative methods. In the second regime, for smaller group velocities, multiple scattering becomes important and influences the propagation properties.

The authors acknowledge Femius Koenderink, Bernard Kaas, Ad Lagendijk, Philippe Lalanne and Thomas Krauss for enlightening discussions. This research is supported by NanoNed, a nanotechnology programme of the Dutch Ministry of Economic Affairs and this work is part of the research program of FOM, which is financially supported by NWO.

---

[1] K. Edagawa, S. Kanoko, and M. Notomi, Phys. Rev. Lett. **100**, 013901 (2008).

[2] A. Berrier *et al.*, Phys. Rev. Lett. **93**, 073902 (2004).

[3] E. Cubukcu *et al.*, Phys. Rev. Lett. **91**, 207401 (2003).

[4] H. Gersen *et al.*, Phys. Rev. Lett. **94**, 073903 (2005).

[5] Y. A. Vlasov, *et al.*, Nature **438**, 65 (2005).

[6] M. Soljačić and J. D. Joannopoulos, Nature Mater. **3**, 211 (2004).

[7] R. D. Meade *et al.*, J. Appl. Phys. **75**, 4753 (1994).

[8] S. Hughes *et al.*, Phys. Rev. Lett. **94**, 033903 (2005).

[9] J. Topolancik, B. Ilic, and F. Vollmer, Phys. Rev. Lett. **99**, 253901 (2007).

[10] J. Bertolotti *et al.*, Phys. Rev. Lett. **94**, 113903 (2005).

[11] D. Gerace and L. C. Andreani, Opt. Lett. **29**, 1897 (2004).

[12] E. Kuramochi *et al.*, Phys. Rev. B **72**, 161318 (2005).

[13] Y. Tanaka *et al.*, Electronics Lett. **40**, 174 (2004).

[14] L. O'Faolain *et al.*, Opt. Express **15**, 13129 (2007).

[15] M. Notomi *et al.*, Phys. Rev. Lett. **87**, 253902 (2001).

[16] Z. Y. Li and K. M. Ho, Phys. Rev. Lett. **92**, 063904 (2004).

[17] T. Baba *et al.*, IEEE J. Sel. Top. Quant. **10**, 484 (2004).

[18] M. Sandtke *et al.*, Rev. Sci. Instrum. **79**, 013704 (2008).

[19] Details regarding the used assumptions on coupling to the probe and its effect on the fitting procedure can be found in the Supplemental Information.

[20] H. Gersen *et al.*, Phys. Rev. Lett. **94**, 123901 (2005).

[21] M. Gurioli *et al.*, Phys. Rev. Lett. **94**, 183901 (2005).

[22] $R^2 = 1 - \frac{\sum_N (\log I_{c,N} - \log I_{m,N})^2}{\sum_N (\langle \log I_{c,N} \rangle_N - \log I_{m,N})^2}$, with $I_{c,N}$ and $I_{m,N}$, being the calculated and measured data, respectively. $\langle\ \rangle_N$ denotes the average.

[23] J. P. Hugonin *et al.*, Opt. Lett. **32**, 2638 (2007).

[24] P. Pottier, M. Gnan, and R. M. De La Rue, Opt. Express **15**, 6569 (2007).

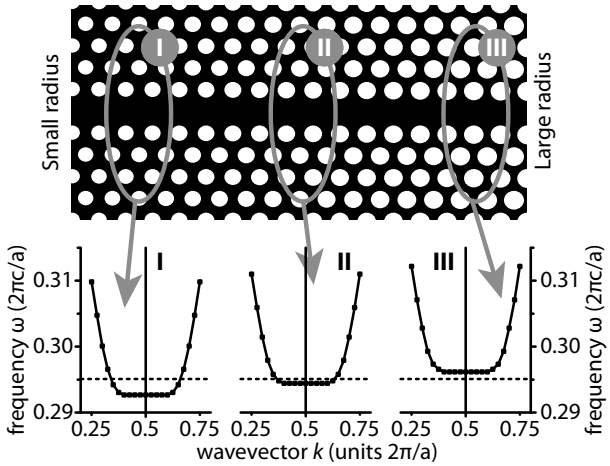

FIG. 1: Schematic representation of the geometry of the chirped waveguide (top). The radius of the holes in the PhC lattice is linearly increased from left to right. The waveguide mode (continuous line) in the dispersion relation shifts up as the hole size increases. Light with a specific optical frequency (dotted line) is therefore allowed to propagate in regions I (with a relatively high v_g) and II (lower v_g), but not in region III. The dispersion relations of regions I, II and III are calculated by 3D FDTD for hole radii of $0.306{\cdot}a$, $0.314{\cdot}a$ and $0.321{\cdot}a$, respectively.

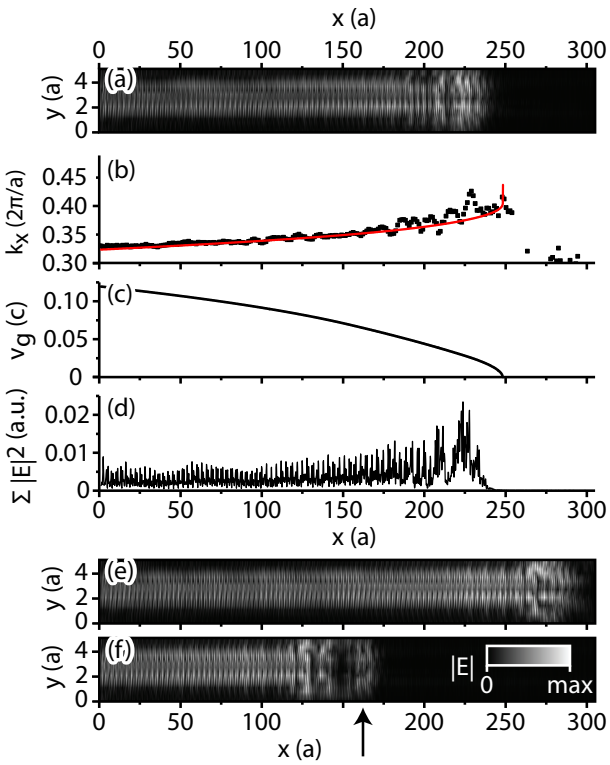

FIG. 2: (a) Near-field measurement on the chirped waveguide at ω=0.2961 (in units $2\pi c/a$). The image represents the measured E-field amplitude. (b) 'Local wavevector' as a function of x-position, obtained from the measurement in (a) (solid points) The solid (red) line depicts the expected wavevector calculated with the dispersion relations of Fig. 1. (c) Group velocity corresponding to the calculated data in (b). (d) Summed intensity ($|E|^2$) over all y points of the image in (a), yielding the total intensity in the waveguide as a function of position x. Data taken from the measurements at ω=0.2961. (e,f) Measured E-field amplitude of the same waveguide and area as in (a), now at ω=0.2973 and 0.2950, respectively. The arrow in (f) indicates a striking disorder-induced resonance.

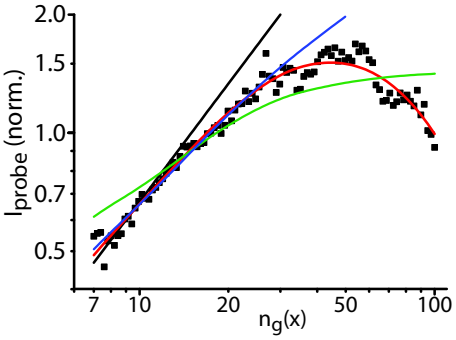

FIG. 3: Intensity detected by the near field probe as a function of the group index n_g, normalized at n_g=20. The data is averaged over 25 measurements, ranging between ω=0.2936 and ω=0.2982. The black line shows a linear relation. The red line represents the best fit to the measurements with $\alpha = 2.84$. The green line represents the best fit using $\alpha = 2$ when its forced to describe all n_g. The blue line is the result of a fit with $\alpha = 2$ for the data points with $n_g < 30$ only.

Supplemental information for:

Two regimes of slow-light losses revealed by adiabatic reduction of group velocity

R.J.P. Engelen[1], D. Mori[2], T. Baba[2], and L. Kuipers[1]

[1] *Center for Nanophotonics, FOM Institute for Atomic and Molecular Physics (AMOLF), Kruislaan 407, 1098 SJ Amsterdam, The Netherlands*

[2] *Yokohama National University, Department of Electrical and Computer Engineering, 79-5 Tokiwadai, Hodogayaku, Yokohama 240-8501, Japan*

Abstract

In the letter, we assumed that the coupling efficiency from the waveguide to the near-field probe is constant. The efficiency does not depend on frequency nor on position. In this supplement, we describe a scenario in which the coupling depends on the local properties of the waveguide. We will show that the conclusions of our manuscript do not change if this scenario were true.

PACS numbers:

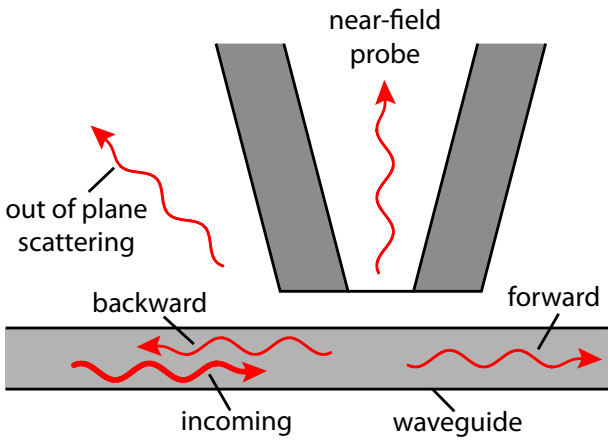

FIG. S 1: Schematic representation of scattering processes near the near-field probe. If the light is scattered near the probe, several channels are available to scatter to: waveguide modes, either forward or backward, or out of the plane: either into the air of into the near-field probe. Note that the largest portion of the incoming light will be transmitted without scattering.

In Fig. S1, we have depicted a schematic representing the possible scattering processes occurring at the location of the near-field probe. An incoming wave that propagates under the near-field probe may be scattered at the probe position. In the figure, we have depicted four channels to which the light can scatter: scattering out-of-plane to radiative modes, into the near-field probe, into the waveguide in the forward direction or the backward direction. The amount of energy scattered to each channel depends on the density of states (DOS) of each channel.

The DOS of the out-of-plane scattering including the coupling to the near-field probe, ρ_{out}, does not change dramatically over the frequency range used in the experiment and can be considered constant. The DOS of the (single-mode) waveguide ρ_{wg}, however is proportional to the group index n_g [S1]. In the experiments, we have investigated a range of group indices between 7 and 100, resulting in the same variation in the DOS of the waveguide.

Given this difference in DOS, we can describe the coupling efficiency into the out-of-plane channels as:

$$\eta_{out} = \frac{\rho_{out}}{\rho_{wg}(n_g) + \rho_{out}}. \tag{1}$$

The coupling efficiency to the near-field probe η_{probe} is a constant fraction of η_{out}.

As a result of the above equation, the coupling to the probe will be reduced if the group index increases. This seems to suggest an alternative explanation for the drop in detected power at large n_g in Fig. 3 (in the letter). We fitted the measured result in this figure by including the above coupling efficiency, now with an additional fitting parameter $\rho_{wg}(1)/\rho_{out}$. Several potential fits in a range of α values are found. To evaluate the quality of these fits, the curve fitting results analyzed in greater detail.

In Fig. S2, the fit goodness R^2 is plotted versus the loss exponent α, for both the model used in the letter (η_{probe} constant) and using the addition described above including the result using Ref. [8]. The model based on a constant coupling efficiency to the probe shows a clear maximum in the range of α=2.7 and α=3.0. The optimum of the extended model does not show a clear maximum. Based on the solid curve in Fig. S2, we estimate a range between α=2.7 and 4.6 to be a reasonable fit to the measured data.

Not all of these α-values are plausible however. At larger α, the loss coefficient A quickly become unacceptably small. At α=3.2 and n_g=7, the corresponding loss would be 0.3 dB/mm,

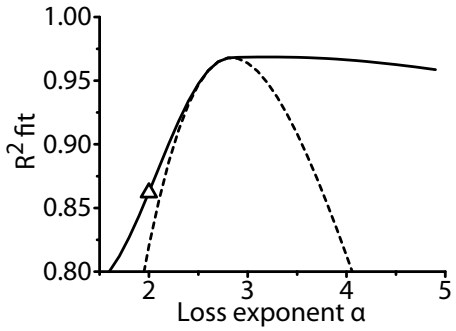

FIG. S 2: Analysis of the goodness R^2 of the fit of the measurement data in Fig. 3, as a function of fit parameter α. For the model with η_{probe} constant (dashed line), using Eq. 1 (solid line) and using Ref. [8] (triangle).

which is roughly equal to the reported record low loss for these waveguides. Given the size polydispersity of the holes of 1 %, record low losses in these structures cannot be expected. Limiting the potential fits to those which would result in reasonable losses for low n_g, we find a loss exponent of 2.9 ± 0.3: the same as the one described in the letter.

[S1] C. Kittel, *Introduction to solid state physics*, (7th ed., Wiley, New York, USA, 1996)